Long Noncoding RNA SNHG4 Remits Lipopolysaccharide-Engendered Inflammatory Lung Damage by Inhibiting METTL3 - Mediated m6A Level of STAT2 mRNA

Si-Xiu Li
Children's Hospital Affiliated to Xi'an Jiaotong University
Wen Yan
Childrens' Hospital Affiliated to Xi'an Jiaotong University
Jian-Ping Liu
Children's Hospital Affiliated to Xi'an Jiaotong University
Yu-Juan Zhao
Children's Hospital Affiliated to Xi'an Jiaotong University
Lu Chen
luchenh@21cn.com

Childrens' Hospital Affiliated to Xi'an Jiaotong University https://orcid.org/0000-0001-9019-2007

Research

Keywords: neonatal pneumonia, lncRNA SNHG4, METTL3, m6A, STAT2

Posted Date: June 16th, 2021

DOI: https://doi.org/10.21203/rs.3.rs-573716/v1

Version of Record: A version of this preprint was published at Molecular Immunology on November 1st, 2021. See the published version at https://doi.org/10.1016/j.molimm.2021.08.008.

Abstract

Background: Emerging evidence suggests that long non coding RNA (lncRNA) small nucleolar RNA host gene 4 (SNHG4) has become a new insight into lipopolysaccharide (LPS) - induced microglia inflammation, its role in neonatal pneumonia (NP) remains to be largely unrevealed.

Methods: RT-qPCR was used to determine SNHG4 and METTL3 expression in the serum from NP patients and normal volunteers, as well as in WI-38 cells treated with LPS. The SNHG4 overexpression vector (pcDNA-SNHG4) was transfected into LPS - treated cells. CCK-8, Transwell, annexin V-FITC/PI and ELISA assays were used to determine cell proliferation, migration, apoptosis and contents of IL-6, TNF-α, SOD and MDA, respectively. The level of SNHG4 in the promoter region of METTL3 was assessed with RIP assay. m^6A quantitative analysis illustrated the m^6A level with or without SNHG4 overexpression or METTL3 silencing. Bioinformatics analysis and RIP-PCR were used to predict and validate YTHDF1 - mediated m^6A levels on signal transducer and activator of transcription 2 (STAT2) mRNA in METTL3 inhibited cells. Then rescue experiments were performed to explore effects of SNHG4 and METTL3 or STAT2 on LPS-treated cell functions. Subsequently, *in vivo* functional experiments were performed to investigate the role of SNHG4 in LPS induced pneumonia in mice.

Results: SNHG4 was downregulated and METTL3 was upregulated in NP patients and LPS-treated cells. SNHG4 overexpression facilitated cell proliferation, migration and SOD concentration, and inhibited apoptosis and IL-6, TNF-α and MDA contents. Mechanistically, SNHG4 bound with METTL3 and downregulated METTL3 expression. Besides, total m^6A modification level was lower in the SNHG4 overexpressed or METTL3 inhibited cells. METTL3 interference reduced m^6A levels of STAT2 mRNA, decreased STAT2 mRNA stability and promoted STAT2 translation level. METTL3 or STAT2 upregulated reversed the effects of SNHG4 overexpression on LPS - treated cell functions.

Conclusions: This study reveals that SNHG4 promotes LPS induced inflammation in human lung fibroblasts and mouse lung tissues *in vitro* and *in vivo* by inhibiting METTL3 - mediated m^6A level of STAT2 mRNA, which may provide a potential therapeutic mechanism for NP.

1 Introduction

Neonatal pneumonia (NP) is one of the ordinary diseases in the neonatal period. It is a vital cause of perinatal death, and its main clinical manifestations include cough and lung fine wet rales[1]. NP is divided into aspiration pneumonia and infectious pneumonia, of which infectious pneumonia accounts for a large proportion[2]. Many factors contribute to the development of infectious neonatal pneumonia, including bacteria, viruses, molds, mycoplasma pneumonia (MP) and other pathogenic factors. The descending infection department caused respiratory infection, the clinical manifestations were no bronchitis, pneumonia and so on. In severe cases, it can accumulate in the brain, heart, liver, and kidney, followed by encephalitis, myocarditis, and hepatitis, among other complications[3]. However, the pathogenesis of neonatal pneumonia is still controversial, and clinical treatment is still difficult.

Therefore, it is of great significance to explore the pathogenesis of neonatal pneumonia from the molecular level. Lipopolysaccharide (LPS), a major bioactive component of Gram-negative bacteria pathogens, can cause severe inflammatory reactions in the lungs[4]. Therefore, LPS induced inflammatory injury is a commonly used model to study the pathogenesis and treatment of NP.

Emerging evidence suggests that lncRNA is a novel insight in various diseases, such as lung injury. In pneumonia, a potential key lncRNA profile in peripheral blood has been identified by lncRNA sequencing[5]. Several lncRNA were further revealed to be associated with lung inflammation. A study revealed that lncRNA-MIAT inhibits p38 MAPK and NF-κB attenuated LPS induced lung inflammatory responses in mice through a pathway that downregulated miR-15[6]. Previous studies show a link between SNHG4 and inflammation. Overexpression of SNHG4 cloud inhibit the expression of inflammatory factors in microglia[7]. Unfortunately, to date, the role of SNHG4 in the inflammatory response in pneumonia remains unclear.

N6-methyladenosine (m^6A) has been reported as the most prevalent internal mRNA modification in eukaryotes, and its role in autoimmunity, inflammation and cancer has attracted close attention. The key enzymes for m^6A methylation modification principally include m^6A methyltransferase (writer), m^6A demethylase (eraser) and m^6A RNA-binding protein (reader)[8]. Methyltransferase-like 3 (METTL3) is a key enzyme of m^6A methylation modification and an important member of the methyltransferase complex including METTL3, METTL4, and Wilms tumor 1-associated protein (WTAP)[9]. It has been demonstrated that m^6A methylation mediated by METTL3 is necessary for inflammatory responses[10]. A research showed that METTL3 deficiency maintained long-chain fatty acid absorption by inhibiting TRAF6-dependent inflammatory responses[11]. Moreover, METTL3 promoted LPS-induced microglial inflammation by activating the TRAF6-NF-κB pathway[12]. Except for ‘writers’ and ‘erasers’, the modification is recognized and bound by m^6A ‘readers’ in mammalian cells, mainly YTHDF1-3 and YTHDC1, 2, which are from YTH-domain family proteins, thus contributing to various biological processes, such as viral infections and tumorigenesis. YTHDF1 (YTH domain family 1) is the most effective m^6A reader that weakens mRNA stability by recognizing and distributing m^6A-containing mRNAs to processing bodies[13]. Recent reports mentioned that YTHDF1 could prevent inflammation in cerebral ischemia / reperfusion injury by m^6A modification of p65 mRNA translation[14]. Nevertheless, the role of METTL3- mediated m^6A / YTHDF1 in NP remains vague up to date.

Based on the above reports, we speculated that SNHG4 and METTL3 might be involved in the progression of NP by regulating inflammatory responses. Therefore, in the present study, we examined whether SNHG4 affects LPS induced injury in WI-38 cells by regulating METTL3, and explored the regulatory correlation between METTL3 mediated m^6A / YTHDF1 and the downstream possible target genes to decode the molecular mechanism by which SNHG4 alleviates lung injury and find a novel target for the treatment of NP.

2 Materials And Methods

2.1 Collection of serum samples

Peripheral venous blood (3 ml) was collected from 15 patients (10 males and 5 females) with neonatal pneumonia; Mean age 10–28 days) and 15 healthy volunteers (10 males and 5 females; Mean age 10–28 days) at Xi'an children's hospital. Patients with other complications or previous anti-inflammatory treatment were excluded. Control blood samples were obtained from persons with normal physical examination results. After collection, blood was centrifuged at 2000 rpm, and then the supernatant was obtained as serum sample and stored at -80°C

2.2 Animals and experimental groups

Forty-eight one week old CD-1 mice were purchased from experimental animal center of Xi'an Jiaotong University (Xian, China). All mice were housed under a 12 h light/dark cycle with constant temperature about 25°C and relative humidity approximating 55%. The mice had free access to food and water for 10 days prior to the experiment. The mice were randomly divided into four groups of 10 mice each. After 10 days, mice received an intraperitoneal injection of 22 mg / ml sodium pentobarbital (diluted in saline) followed by 167 μM LPS (60 μL) Saline solution was instilled into the oral cavity through the posterior pharyngeal wall. Pinch the nares quickly and hold for 30 seconds, model is successful when all fluid is absorbed into the nasal cavity, and slight tracheal rales appear. Lentiviral vectors containing pcDNA-SNHG4 (150 μM) or pcDNA-3.1 were intratracheally injected into mice. Twenty-one days after establishing the model, mice were intraperitoneally injected with 3% sodium pentobarbital and euthanized by overdose anesthesia at a dose of 90 mL / Kg, and organs and tissues were removed for follow-up studies. In addition, macrophages and neutrophils in alveolar lavage fluid were collected as previously described. The protocol of this study was approved by the animal care and use Committee of the children's Hospital of Xi'an Jiaotong University.

2.3 Cell Lines and Culture

Human lung fibroblasts (WI-38) were purchased from American Type Culture Collection (ATCC, Manassas, VA, USA). The cells were maintained in Dulbecco's Modified Eagle Medium (DMEM) (Gibco, Rockville, MD) supplemented with 10% fetal bovine serum (FBS) (HyClone, Salt Lake City, UT) and 1% penicillin-streptomycin (Sigma, St. Louis, MO, USA) at 37°C in a controlled humidified atmosphere with 5% CO_2. 2×10^5 cells were plated in 6-well plates and incubated. LPS (Sigma, St. Louis, MO) was diluted by DMEM to 10 ng/mL and the processing time was 6 hr.

2.4 Cell transfection

The pcDNA-SNHG4, pcDNA-METTL3, pcDNA-STAT2, pcDNA-YTHDF1 and METTL3 siRNA were all obtained from GenePharma Co., Ltd. (Shanghai, China). Before transfection, WI-38 cells were digested with 1% trypsin treatment. After being counted in a blood counting chamber, the cells were plated onto six-well culture plates for 24 hours and then transfected at 40%-60% confluence. All transfection was performed with Lipofectamine®3000 (Thermo, Waltham, MA, USA) according to manufacturer's instructions. At 48 hours post-transfection, cells were harvested and subjected to next analyses.

2.5 Quantitative real-time polymerase chain reaction (RT-qPCR)

Total RNA from clinical samples or cultured cells was extracted by using Trizol reagent (Invitrogen, Carlsbad, CA, USA) with the manufacturer's instructions. Reverse transcription was carried out by using Prime Script RT reagent Kit (Takara, Dalian, China). Real-time PCR analyses were conducted with the SYBR Premix Ex Taq II (Takara, Dalian, China) on an ABI 7500 Real-Time PCR System (Applied Biosystems, Foster City, CA) under the following conditions: 95°C for 1 min, and then 95°C for 20 s, 56°C for 10 s and 72°C for 15 s for 35 cycles. The PCR conditions are as follows: 2 μL of cDNA was added to 10 μL of the 2× SYBR green PCR master mix with 0.4 μL of Taq polymerase enzyme (RiboBio Co., Ltd, Guangzhou, China), 0.8 μL of each primer and 6 μL of ddH_2O to a final volume of 20 μL. The primer sequences were as follows: METTL3 forward, 5'-ACC TAT GCT GAC CAT TCC AAG-3'; and reverse, 5'-CTG TTG GTT CAG AAG GCT CTC-3'; LncRNA SNHG4 forward, 5'- GCA ACC CCT TCA GCT CTC TT -3'; and reverse, 5'- CCC TTT GAG CCC TTG GTA GG -3'; STAT2 forward, 5'- AAA TAG CTT GCC CAG GCC AT-3'; and reverse, 5'- AGG CAG CAG AGG AGG GAA TA-3'; GAPDH forward, 5'-TGA CCA CAG TCC ATG CCA TCA C-3'; reverse: 5'-GCC TGC TTC ACC ACC TTC TTG A-3'. The relative expression was normalized to glyceraldehyde 3-phosphate dehydrogenase (GAPDH) and calculated by the $2^{-\Delta\Delta CT}$ method.

2.6 Western blotting

The cells were washed twice with ice-cold PBS and lysed by using RIPA lysis buffer (CW Biotech, Beijing, China) supplemented with protease inhibitor (Roche Diagnostics, Basel, Switzerland). Then the protein concentration was measured by BCA protein assay kit (Thermo Fisher Scientific, Waltham, MA, USA). Equal amount of protein was subjected to 10% SDS-PAGE at 70 V for 30 min then 120 V for 90 min. And the protein bands were transferred to PVDF membranes at 300 mA for 2 h. The membranes were blocked with 5% skim milk for 2 h at room temperature, and then incubated with the following primary antibodies: rabbit polyclonal anti-β-actin antibody (1:1000, Abcam, ab8227), rabbit monoclonal anti-METTL3 antibody (1:1000, Abcam, ab195352), rabbit polyclonal anti-STAT2 antibody (1:2000, Abcam, ab32520). Then, the membranes were incubated with horseradish peroxidase (HRP)-conjugated goat anti-rabbit IgG (1:3000, Abcam, ab6721) for 1 h at room temperature. β-actin was used as an endogenous control. The bands were visualized by using an ECL Plus Chemiluminescence Reagent Kit (Pierce, Rockford, IL, USA) and were photographed by a chemiluminescence imaging system. Image J software was used to quantify the band densities.

2.7 Cell proliferation assay

The Cell Counting Kit-8 (CCK-8) assay (Sigma-Aldrich, St. Louis, MO, USA) was performed to detect WI-38 cell proliferation. In brief, WI-38 cells were seeded into 96-well microplates. After incubation for 0, 24, 48 and 72 h, 10 μL of CCK-8 solution was added to each well and incubated with HL-1 cells for another 2 h at 37°C in a humidified atmosphere with 5% CO_2. A microplate reader (Molecular Devices, Shanghai, China) was used to measure the absorbance of each well at 450 nm.

2.8 Cell apoptosis assay

Annexin V-FITC/PI double staining was used to analyze apoptosis on a flow cytometer (BD Bioscience, San Jose, CA, USA). After 48 h of transfection, the WI-38 cells were detached with EDTA-free trypsin and collected afterwards. The cells were centrifuged for 5 min at 4°C at 1000 rpm, and the supernatant was discarded. Apoptosis was detected by an Annexin V-FITC/PI Apoptosis Detection Kit (Beijing Solarbio Science & Technology, Beijing, China). The WI-38 cells were suspended in a mixture of AnnexinV-FITC and binding buffer (1:40) and incubated at room temperature for 30 min. A mixture of PI and binding buffer (1:40) was then added and shaken, followed by incubation at room temperature for 15 min. Fluorescence was detected by a flow cytometer, and the apoptosis rate was calculated and determined.

2.9 Transwell migration assay

The cell motility was detected by treatment with 8.0-μm chamber plates. Firstly, cells were planted into the 8.0 μm chamber plates, then 300 μL of serum-free DMEM medium was added to the upper compartment of the chamber, and 500 μL of DMEM medium supplemented with 10% FBS was added to the lower chamber for 48 h incubation. Then, the non-migratory cells on the upper side of the chamber were suspended with a cotton swab, and then the migratory cells were fixed in 4% paraformaldehyde and stained with a crystal violet solution. We stained infiltrating cells using an Olympus IX70 inverted microscope (Olympus Corp, Tokyo, Japan) and randomly selected the best six fields of view, and each experiment was repeated three times.

2.10 Enzyme-linked immunosorbent assay (ELISA)

WI-38 cells and mouse lung tissues were assayed for Interleukin-6 (IL-6), tumor necrosis factor alpha (TNF-α), superoxide dismutase (SOD) and malondialdehyde (MDA) contents with ELISA kits (Thermo Fisher Scientific, Waltham, Ma, USA), according to the manufacturer's instructions.

2.11 RNA Immunoprecipitation (RIP)

Total RNA was isolated from WI-38 cells by using Trizol. Anti-m^{6}A antibody (Abcam, ab151230) (or anti-METTL3 antibody or anti-YTHDF1 antibody) and anti IgG (Abcam, ab172730) were conjugated to protein A / G magnetic beads in IP buffer (140 mM NaCl, 1% NP-40, 2 mm EDTA, 20 mm Tris pH.7.5) overnight at 4°C. Total RNA was incubated with antibodies in IP buffer, and precipitated RNA was then eluted from the beads. Finally, precipitated RNA and input total RNA were eluted and reverse transcribed for RT-qPCR. Relative fold enrichment was calculated with the $2^{-\Delta\Delta CT}$ method.

2.12 Total m ^{6} A Measurement

Total RNA was isolated by TRIzol (Thermo Fisher, USA) according to the manufacturer's instructions. The relative content of m^{6}A in the total RNA was measured by using the EpiQuik m^{6}A RNA Methylation Quantification Kit (Colorimetric) (P-9005, Epigentek, USA) according to the manufacture's instruction. In

brief, 200 ng RNA were administrated with the solution containing the anti-m^6A antibody. The m^6A levels were quantified by using the colorimetrical analysis via absorbance at 450 nm.

2.13 Statistical Analysis

All statistical analyses were performed with the SPSS software (ver.22.0; SPSS, Chicago, IL). All data were shown as mean ± SEM. Student's t-test was performed for the comparison between two groups, and analysis of variance (ANOVA) was performed for comparison among groups. P 0.05 was considered as statistically significant difference.

3 Results

3.1 LncRNA SNHG4 was downregulated in the serum of patients with pneumonia and LPS-induced cell model of pneumonia

We examined a total of 30 serum samples including 15 patients with pneumonia and 15 healthy controls. As shown in Fig. 1A, the expression level of SNHG4 was abundantly decreased in the serum from patients with pneumonia compared to the controls. LPS was used to treat human lung fibroblasts to establish an *in vitro* cellular model of pneumonia. The dosage of LPS treatment was determined in WI-38 cells. After LPS stimulation (5, 10, and 20 μg / ml) for 24 hours, SNHG4 levels were attenuated with increasing LPS concentrations (Fig. 1B). These results indicated that the downregulated expression of SNHG4 might be associated with progression of pneumonia.

3.2 Overexpression of SNHG4 attenuated LPS-induced inflammation and injury in cells

To explore the effect of SNHG4 in cell model of pneumonia in human lung fibroblast cells, WI-38 cells transfected with pcDNA-SNHG4 or pcDNA-3.1 were treated with 10 μg/mL of LPS. The results in Fig. 2A revealed that pcDNA-SNHG4 transfection could significantly increase SNHG4 expression in LPS-induced WI-38 cells. Furthermore, SNHG4 overexpression facilitated LPS-treated WI-38 cell proliferation and migration and restrained apoptosis (Fig. 2B-2E, $P < 0.01$). The levels of both IL-6 and TNF-α were increased in WI-38 cells under LPS treatment, which was reversed by SNHG4 upregulation (Fig. 2F, $P < 0.01$). Moreover, compared with LPS alone treatment group, the level of SOD was increased and MDA was decreased significantly after overexpression of SNHG4 in LPS-treated cells (Fig. 2G-2H, $P < 0.01$). These results suggested a protective role of SNHG4 overexpression in LPS-induced cell model of pneumonia in human lung fibroblast cells by reducing cell apoptosis and inflammation.

3.3 SNHG4 negatively regulated METTL3 expression in human lung fibroblast WI-38 cells.

To further investigate the underlying mechanism of SNHG4 in the regulation of pneumonia progression, we predicted the downstream targets of SNHG4 by online bioinformatic tool and found that SNHG4 might bind to the METTL3 promoter region. Interestingly, we found that the expression of METTL3 in pneumonia patient serum and LPS incubated cells was significantly higher than that in normal serum and cells (Fig. 3A and 3B, $P < 0.01$). We used Pearson correlation test to evaluate the relationship between SNHG4 and METTL3, and the findings suggested that there was a strongly negative correction between SNHG4 and METTL3 levels (Fig. 3C, $P < 0.01$). Besides, RIP results showed that SNHG4 could combine with METTL3 in WI-38 cells (Fig. 3D, $P < 0.01$). The m^6A quantitative analysis unveiled that the percentage of m^6A content in the total RNA was markedly decreased in the SNHG4 overexpressed cells in the present of LPS treatment (Fig. 3D, $P < 0.01$). The mRNA level of METTL3 in WI-38 cells were memorably upregulated after LPS treatment, whereas SNHG4 overexpression could reversed this result (Fig. 3F, $P < 0.01$). Overall, these findings concluded that SNHG4 inhibited METTL3 expression upregulation in in pneumonia patient serum and LPS-treated cells, which was also correlated with m^6A content.

3.4 Overexpression of SNHG4 alleviated LPS-induced inflammatory damage by inhibiting METTL3 expression

To elucidate whether SNHG4 functions by regulating METTL3, rescue experiments were performed with co-transfection of pcDNA-SNHG4 with pcDNA-METTL3 plasmid. The efficiency of pcDNA-METTL3 on its expression level in WI-38 cells was verified by Western blotting (Fig. 4A and 4B). The results indicated that the pcDNA-METTL3 significantly restrained the proliferation, migration and SOD content, as well as promoted apoptosis, inflammatory factor contents and MDA concentration of WI-38 cells and reversed the effects on these processes induced by SNHG4 upregulation (Fig. 4C-4K, $P < 0.05$). Collectively, these data demonstrate that METTL3 exerts an injury promoting effect on WI-38 cells and serves a crucial function downstream of SNHG4.

3.5 Interference of METTL3 decreases the m^6A level of STAT2 mRNA

As shown in Fig. 5A, with the help of online bioinformatics tools, we found that there were m^6A binding sites on STAT2 mRNA. The m^6A binding sequence in the STAT2 promoter region is ‘GGACT’. The m^6A quantitative analysis revealed that the m^6A global methylation quantity is downregulated in the METTL3 inhibited WI-38 cells (Fig. 5B, $P < 0.01$). RIP-qPCR revealed that METTL3 silencing significantly reduced SOCS3 mRNA enrichment precipitated by the antibody (Fig. 5C, $P < 0.01$). The efficiency of METTL3 siRNA on its expression level in WI-38 cells was verified by Western blotting (Fig. 5D-5E, $P < 0.01$). Moreover, METTL3 knockdown observably decreased SOCS3 mRNA and protein levels (Fig. 5D and 5F-5G, $P < 0.01$). YTH m^6A RNA-binding protein 1 (YTHDF1) is known to promote translation of m^6A methylated transcripts[15]. The expression of STAT2 appeared to be promoted by m^6A methylation, which raises the possibility that it is a target of YTHDF1. As expected, RIP-qPCR analysis revealed that

STAT2 is a target gene of YTHDF1 (Fig. 5H). Overexpression of YTHDF1 can partially rescue the reduced STAT2 mRNA and protein expression levels caused by METTL3 knockdown in WI-38 cells (Fig. 5I-5J), confirming that YTHDF1 is involved in regulation of STAT2.

3.6 Overexpression of STAT2 reversed the ameliorative effect of SNHG4 upregulated on LPS-induced inflammatory damage

As STAT2 is a structural target that functions downstream of METTL3 and SNHG4, we further evaluated whether SNHG4 and STAT2 are functionally associated, pcDNA-SNHG4 and pcDNA-STAT2 was transfected alone or together into LPS-treated WI-38 cells. The efficiency of pcDNA-STAT2 on its expression level in WI-38 cells was verified by Western blotting (Fig. 6A and 6B). Subsequently, with CCK-8, Annexin V-FITC/PI, Transwell and ELISA assays, STAT2 overexpression was demonstrated to inhibit the proliferation, migration and SOD content, as well as facilitate the apoptosis, inflammatory factor concentration and MDA content of WI-38 cells. Further, we observed that the inhibitory effects on malignant biological behaviors and inflammatory factors secretion after SNHG4 overexpression could be largely blocked by STAT2 overexpression (Fig. 6C-6K). Collectively, our data suggest that the inhibitory role of SNHG4 in maintaining LPS induced injury was largely dependent on the METTL3/STAT2 axis.

3.7 Overexpression of SNHG4 alleviates LPS-induced inflammation and injury in mice

To further investigate, we intratracheally injected SNHG4 overexpression vector into mice. Consistent with in vitro findings, compared with the control group, LPS treatment prominently inhibited SNHG4 expression and promoted the protein levels of METTL3 and STAT2, which were observably reversed by SNHG4 upregulation (Fig. 7A-7D, $P < 0.01$). As well, compared with the LPS treated group, the overexpression of SNHG4 inhibited inflammatory factor expression and MDA concentration, and restored SOD content (Fig. 7E-7H, $P < 0.05$). In addition, LPS stimulation increased wet dry mass ratio (W/D) and myeloperoxidase (MPO) contents of isolated lungs, while pcDNA-SNHG4 injection decreased W/D and MPO, indicating that SNHG4 could suppressed pulmonary edema (Fig. 7I-7J, $P < 0.05$). Then, we collected and counted the macrophages and neutrophils in the alveolar lavage fluid, and LPS injection promoted the number of macrophages and neutrophils, while SNHG4 overexpression inhibited the aggregation of macrophages and neutrophils (Fig. 7K-7L, $P < 0.01$).

4 Discussion

NP morbidity and mortality rate are very high, seriously impact on the physical health of newborn[4]. In this study, LPS was used for inducing WI-38 cells to establish a pneumonia inflammatory damage model. First, we found that LPS meaningfully inhibited cell viability and migration, enhanced apoptosis, and increased the levels of inflammatory factors IL-6 and TNF-α and oxidative stress. This is consistent with

previous findings. Zhang et al. Found that LPS induced WI-38 injury model could inhibit cell viability and enhance cell apoptosis at the cellular level, and increase the expression levels of Bax and cleaved-caspase-3 and the contents of IL-6 and MCP-1 at the molecular level[16]. Further studies revealed that LPS negatively regulated SNHG4 expression. Several lncRNAs have been proposed to regulate LPS induced cell models in pneumonia. For instance, a research reported that lncRNA XIST was highly expressed in patients with acute stage of pneumonia. Knockdown of XIST remarkably alleviated LPS-induced cell injury through increasing cell viability and inhibiting apoptosis and inflammatory cytokine levels through regulating JAK/STAT and NF-κB pathways[17]. lncRNA MIAT2 protected WI-38 cells from LPS injury and apoptosis through miR-15 / p38MAPK crosstalk, and ultimately affected the development of pneumonia[6]. Moreover, another study found that SNHG4 could regulate STAT2 and repress inflammation by adsorbing miR-449c-5p in microglia during cerebral ischemia-reperfusion injury[7]. Here, we observed that SNHG4 expression in serum of patients with pneumonia was significantly downregulated, and pcDNA-SNHG4 pre-transfection prominently inhibited the negative effects of LPS treatment on WI-38 cells and mouse lung tissue, suggesting that SNHG4 may participate in the anti LPS induced inflammatory injury *in vitro* and *in vivo*. In addition, we found that SNHG4 could bind and negatively regulate the expression of METTL3.

Recently accumulating data showed that METTL3, a methylation regulator of m^6A, was dysregulated in various types of tumor and inflammatory diseases by affecting cell proliferation, invasion and apoptosis. For example, LPS could enhance the expression and biological activity of METTL3 in macrophages, while overexpression of METTL3 significantly attenuated the inflammatory response induced by LPS in macrophages[18]. Overexpression of METTL3 promoted the activation of the TRAF6-NF-κB pathway in an m^6A-dependent manner, further inhibiting NF-κB attenuated METTL3-mediated microglial activation and promoting LPS-induced microglial inflammation[12]. Notably, previous studies mainly focused on the effects of METTL3 on mRNA stability and translation, and little is known about whether it is regulated by lncRNAs to participate in disease initiation and progression. We found that LPS could enhance METTL3 expression at the mRNA levels in a dose-dependent manner in WI-38 cells. Besides, SNHG4 inhibited METTL3 expression upregulation in in NP patient serum and LPS-treated cells, which was also correlated with m^6A content. Specifically, in WI-38 cells, SNHG4 upregulation was accompanied by decreased mRNA stability and protein expression of METTL3 and its associated m^6A methylation levels, which resulted in promotion of cell proliferation as well as inhibition of apoptosis. A previous study revealed that LNC942 specifically binds to the METTL14 protein and a specific motif 'GCAGGG' within the sequence. Thereafter, METTL14 regulated by LNC942 promotes the stability and expression of m^6A methylation levels and its target genes, such as CXCR4 and CYP1B1[19]. In this study, the promotion was almost restored by exposure to overexpression of SNHG4 and METTL3 *in vitro*, followed by reversal of the expression patterns of the above genes.

Janus kinase (JAK) / signal transducer and activator of transcription (STAT) pathway plays an important role in cytokine mediated biological response and is a classic inflammation related pathway. STAT may contribute to the development of acute lung injury inflammation. A research revealed that Azd1480,

STAT2 inhibitor, could significantly reduce lung injury, reduce protein leakage and inhibit inflammatory cytokines release[20]. Cooperative networks of posttranscriptional modification pathways may ultimately regulate cell fate determination or stress by coordinating mRNA stability, translation efficiency, and splicing of transcripts that maintain cell type specific proteomes. m^6A modification is a dynamic and reversible process mediated by three m^6A key elements (‘Writers’, ‘Erasers’ and ‘Readers’). m^6A reader proteins are also necessary in this process, including YTHDF1.The current study showed that METTL3 was responsible for catalytically installed m^6A, and YTHDF1 were identified as ' readers' of m^6A to regulate the stability of m^6A bearing transcripts. YTHDF1 can destabilize m^6A-containing mRNA to control the expression of key genes in multiple biological processes[21]. A study has found that METTL3 recruited YTHDF1 to enhance HK2 stability, thus promoting the Warburg effect in cervical cancer, which may facilitate new insights into cervical cancer treatment[22]. In this study, we found that m^6A modification regulated STAT2 expression in a YTHDF1 orchestrated manner. Mechanistically, YTHDF1 recognizes and binds m^6A-containing mRNA of STAT2, promotes translation and protein expression. Similarly, a recent study demonstrated that silencing METTL3 significantly promotes adipogenesis in porcine BMSCs by targeting the JAK1/STAT5/C/EBPβ pathway through an m^6A-YTHDF1-dependent regulatory mode[23]. Further, we found that STAT2 was modified by m^6A, and RIP-qPCR confirmed that STAT2 was a target of YTHDF1. Overexpression of YTHDF1 can partially rescue the reduced STAT2 mRNA and protein expression levels caused by METTL3 knockdown in WI-38 cells. A previous study has shown that METTL3 promoted STAT3 protein expression by regulating the translation of m^6a- YTHDF1 dependent pathway[24], which further confirmed our conclusion.

In summary, we found that SNHG4 was downregulated in the serum of patients with NP and its overexpression could inhibit LPS induced inflammatory injury in human lung fibroblasts and mouse lung tissue. The molecular mechanism underlying this protective effect was achieved by suppression of METTL3-mediated m^6A modification levels of YTHDF1-dependent STAT2 mRNA. These findings contribute to a more extensive and in-depth understanding of the mechanism of lncRNAs in the occurrence and development of NP, and lay the foundation for finding a new target for the treatment of NP.

5 Abbreviations

Neonatal pneumonia (NP), small nucleolar RNA host gene 4 (SNHG4), lipopolysaccharide (LPS), N6-methyladenosine (m^6A), YTHDF1 (YTH domain family 1), Methyltransferase-like 3 (METTL3), fetal bovine serum (FBS), Dulbecco's Modified Eagle Medium (DMEM), The Cell Counting Kit-8 (CCK-8), optical density (OD), immunoglobulin G (IgG), RNA Immunoprecipitation (RIP), superoxide dismutase (SOD), malondialdehyde (MDA), interleukin-6 (IL-6), tumor necrosis factor-alpha (TNF-α), enzyme-linked immunosorbent assay (ELISA), long non-coding RNA (lncRNA), Standard Error of Mean (SEM).

6 Declarations

Funding

Not applicable

Competing interests

The authors declare that they have no competing interests.

Availability of data and materials

The datasets used during the present study are available from the corresponding author on reasonable request.

Code availability

Not applicable

Authors' contributions

Si-Xiu Li wrote the manuscript. Lu Chen designed this study. Si-Xiu Li and Wen Yan performed the experimental work. Jian-Ping Liu provided the majority of statistical analysis as well as provided the figures and tables for the manuscript. Yu-Juan Zhao collected a large amount of data for the dataset. All authors read and approved the final manuscript.

Ethics approval and consent to participate

This research was approved by the Medical Ethics Committee of the Xi'an Jiaotong University. All patients had read and signed the informed consent.

Acknowledgements

No applicable.

7 References

[1] Wang S, Guo L, Chen L, Liu W, Cao Y, Zhang J, et al. A Case Report of Neonatal 2019 Coronavirus Disease in China. Clin Infect Dis. 2020;71(15):853-857.

[2] Li N, Han L, Peng M, Lv Y, Ouyang Y, Liu K, et al. Maternal and Neonatal Outcomes of Pregnant Women With Coronavirus Disease 2019 (COVID-19) Pneumonia: A Case-Control Study. Clin Infect Dis. 2020;71(16):2035-2041.

[3] Shalish W, Lakshminrusimha S, Manzoni P, Keszler M, and Sant'Anna GM. COVID-19 and Neonatal Respiratory Care: Current Evidence and Practical Approach. Am J Perinatol. 2020;37(8):780-791.

[4] Juan J, Gil MM, Rong Z, Zhang Y, Yang H, and Poon LC. Effect of coronavirus disease 2019 (COVID-19) on maternal, perinatal and neonatal outcome: systematic review. Ultrasound Obstet Gynecol. 2020;56(1):15-27.

[5] Huang S, Feng C, Chen L, Huang Z, Zhou X, Li B, et al. Identification of Potential Key Long Non-Coding RNAs and Target Genes Associated with Pneumonia Using Long Non-Coding RNA Sequencing (lncRNA-Seq): A Preliminary Study. Med Sci Monit. 2016;22:3394-3408.

[6] Zhang H, Zhao J, and Shao P. Long noncoding RNA MIAT2 alleviates lipopolysaccharide-induced inflammatory damage in WI-38 cells by sponging microRNA-15. J Cell Physiol. 2020;235(4):3690-3697.

[7] Zhang S, Sun WC, Liang ZD, Yin XR, Ji ZR, Chen XH, et al. LncRNA SNHG4 Attenuates Inflammatory Responses by Sponging miR-449c-5p and Up-Regulating STAT6 in Microglial During Cerebral Ischemia-Reperfusion Injury. Drug Des Devel Ther. 2020;14:3683-3695.

[8] Zhang H, Shi X, Huang T, Zhao X, Chen W, Gu N, et al. Dynamic landscape and evolution of m6A methylation in human. Nucleic Acids Res. 2020;48(11):6251-6264.

[9] Wang CX, Cui GS, Liu X, Xu K, Wang M, Zhang XX, et al. METTL3-mediated m6A modification is required for cerebellar development. PLoS Biol. 2018;16(6):e2004880.

[10] Han J, Wang JZ, Yang X, Yu H, Zhou R, Lu HC, et al. METTL3 promote tumor proliferation of bladder cancer by accelerating pri-miR221/222 maturation in m6A-dependent manner. Mol Cancer. 2019;18(1):110.

[11] Zong X, Zhao J, Wang H, Lu Z, Wang F, Du H, et al. Mettl3 Deficiency Sustains Long-Chain Fatty Acid Absorption through Suppressing Traf6-Dependent Inflammation Response. J Immunol. 2019;202(2):567-578.

[12] Wen L, Sun W, Xia D, Wang Y, Li J, and Yang S. The m6A methyltransferase METTL3 promotes LPS-induced microglia inflammation through TRAF6/NF-κB pathway. Neuroreport. 2020.

[13] Hou J, Zhang H, Liu J, Zhao Z, Wang J, Lu Z, et al. YTHDF2 reduction fuels inflammation and vascular abnormalization in hepatocellular carcinoma. Mol Cancer. 2019;18(1):163.

[14] Zheng L, Tang X, Lu M, Sun S, Xie S, Cai J, et al. microRNA-421-3p prevents inflammatory response in cerebral ischemia/reperfusion injury through targeting m6A Reader YTHDF1 to inhibit p65 mRNA translation. Int Immunopharmacol. 2020;88:106937.

[15] Chen XY, Liang R, Yi YC, Fan HN, Chen M, Zhang J, et al. The m(6)A Reader YTHDF1 Facilitates the Tumorigenesis and Metastasis of Gastric Cancer via USP14 Translation in an m(6)A-Dependent Manner.

Front Cell Dev Biol. 2021;9:647702.

[16] Zhao YJ, Chen YE, Zhang HJ, and Gu X. LncRNA UCA1 remits LPS-engendered inflammatory damage through deactivation of miR-499b-5p/TLR4 axis. IUBMB Life. 2021;73(2):463-473.

[17] Zhang Y, Zhu Y, Gao G, and Zhou Z. Knockdown XIST alleviates LPS-induced WI-38 cell apoptosis and inflammation injury via targeting miR-370-3p/TLR4 in acute pneumonia. Cell Biochem Funct. 2019;37(5):348-358.

[18] Wang J, Yan S, Lu H, Wang S, and Xu D. METTL3 Attenuates LPS-Induced Inflammatory Response in Macrophages via NF-κB Signaling Pathway. Mediators Inflamm. 2019;2019:3120391.

[19] Sun T, Wu Z, Wang X, Wang Y, Hu X, Qin W, et al. LNC942 promoting METTL14-mediated m(6)A methylation in breast cancer cell proliferation and progression. Oncogene. 2020;39(31):5358-5372.

[20] Liu Q, Xie W, Wang Y, Chen S, Han J, Wang L, et al. JAK2/STAT1-mediated HMGB1 translocation increases inflammation and cell death in a ventilator-induced lung injury model. Lab Invest. 2019;99(12):1810-1821.

[21] Liu T, Wei Q, Jin J, Luo Q, Liu Y, Yang Y, et al. The m6A reader YTHDF1 promotes ovarian cancer progression via augmenting EIF3C translation. Nucleic Acids Res. 2020;48(7):3816-3831.

[22] Wang Q, Guo X, Li L, Gao Z, Su X, Ji M, et al. N(6)-methyladenosine METTL3 promotes cervical cancer tumorigenesis and Warburg effect through YTHDF1/HK2 modification. Cell Death Dis. 2020;11(10):911.

[23] Yao Y, Bi Z, Wu R, Zhao Y, Liu Y, Liu Q, et al. METTL3 inhibits BMSC adipogenic differentiation by targeting the JAK1/STAT5/C/EBPβ pathway via an m(6)A-YTHDF2-dependent manner. Faseb j. 2019;33(6):7529-7544.

[24] Wu R, Liu Y, Zhao Y, Bi Z, Yao Y, Liu Q, et al. m(6)A methylation controls pluripotency of porcine induced pluripotent stem cells by targeting SOCS3/JAK2/STAT3 pathway in a YTHDF1/YTHDF2-orchestrated manner. Cell Death Dis. 2019;10(3):171.

Figures

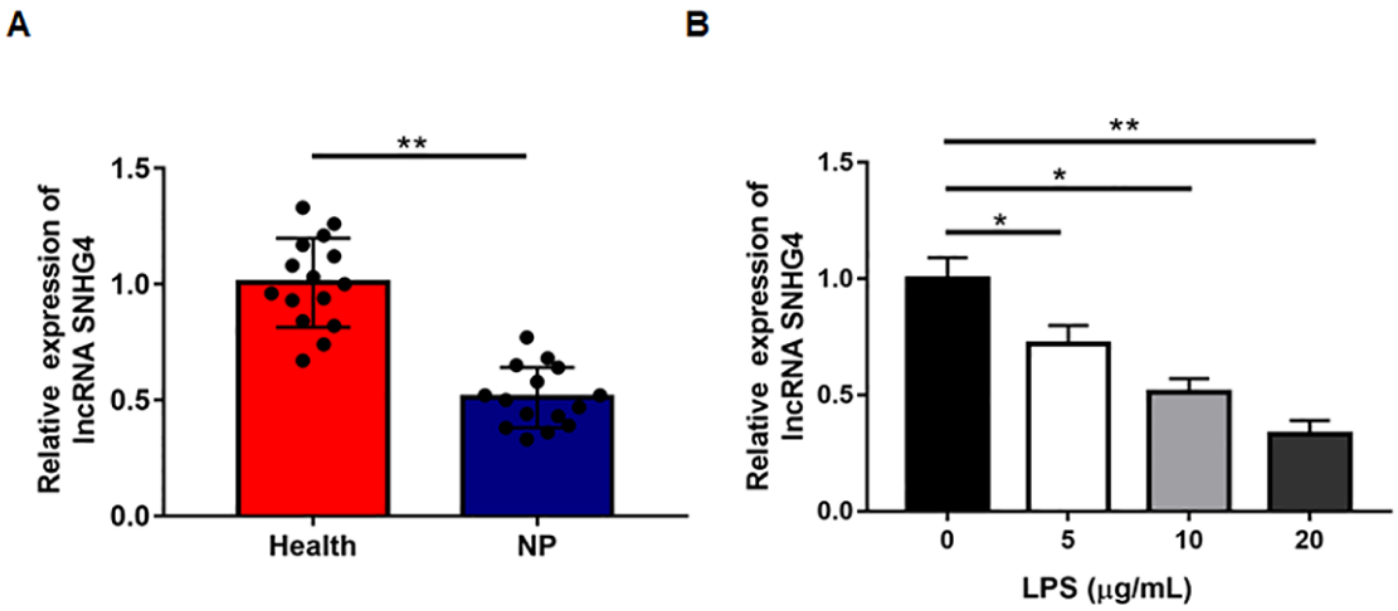

Figure 1

The expression of lncRNA SNHG4 (SNHG4) in patients with pneumonia and LPS-induced human lung fibroblast cells. A-B: RT-qPCR was used to detect SNHG4 level in the serum of patients with pneumonia (n = 15) and healthy controls (n = 15), and in WI-38 cells under LPS treatment (0, 5, 10, and 20 μg/mL) for 24 h. Data were presented as mean ± SEM. N=5, *P < 0.05, **P < 0.01.

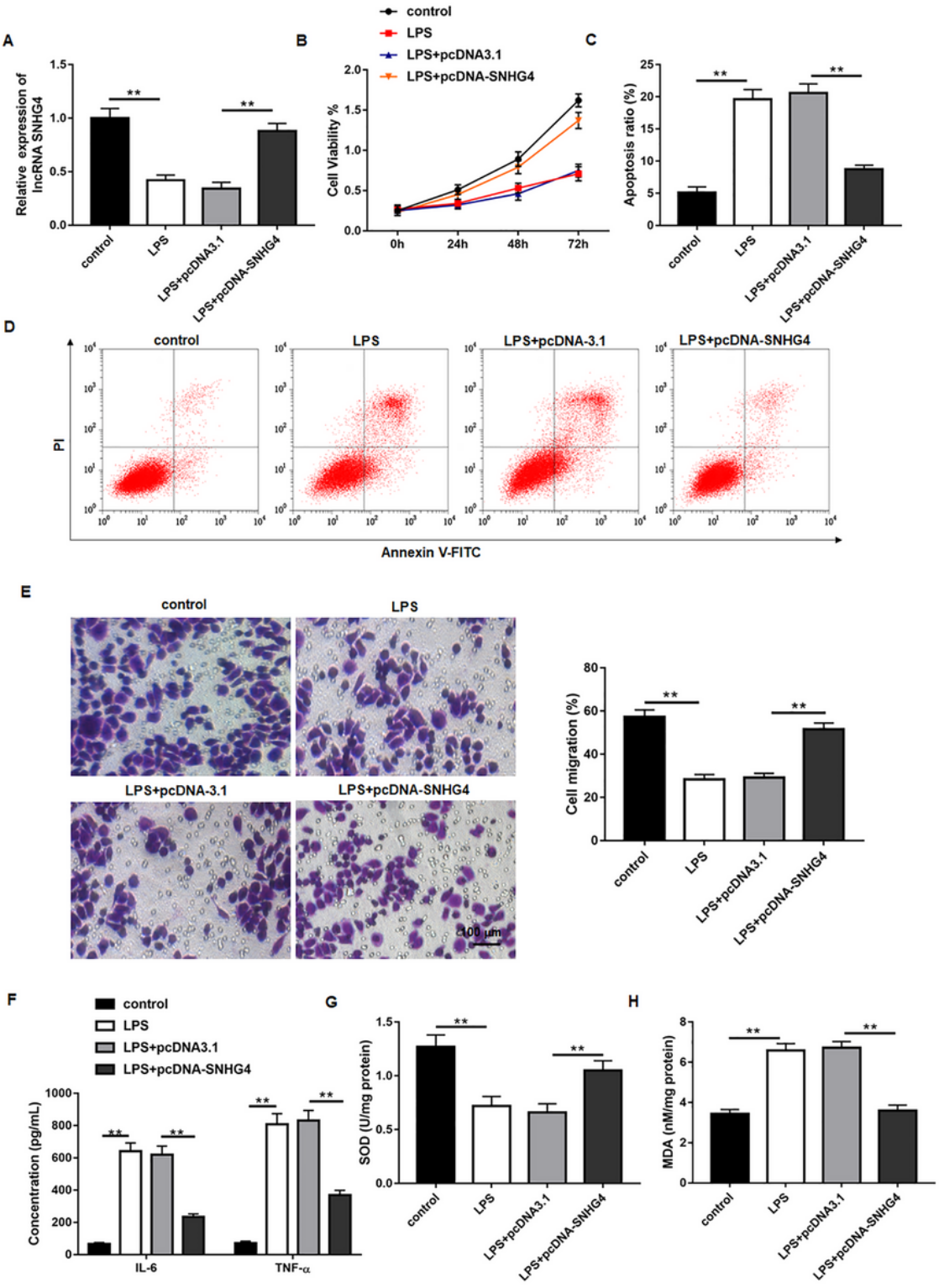

Figure 2

Overexpression of SNHG4 attenuated LPS-induced inflammation and injury in cells WI-38 cells were transfected with pcDNA-SNHG4 or pcDNA-3.1, and then treated with 10 μg/mL of LPS for 24 h. A: After LPS stimulation, RT-qPCR was used to determine the levels of SNHG4 in WI-38 cells. B: The cell proliferation of WI-38 cells was detected by CCK-8 assay. C-D: The cell apoptosis ratio was determined by flow cytometry. E: The cell migration ability was determined with Transwell assay. F-H: The contents of IL-

6, TNF-α, SOD and MDA was detected by ELISA in WI-38 cells. Data were presented as mean ± SEM. N=5, **P < 0.01.

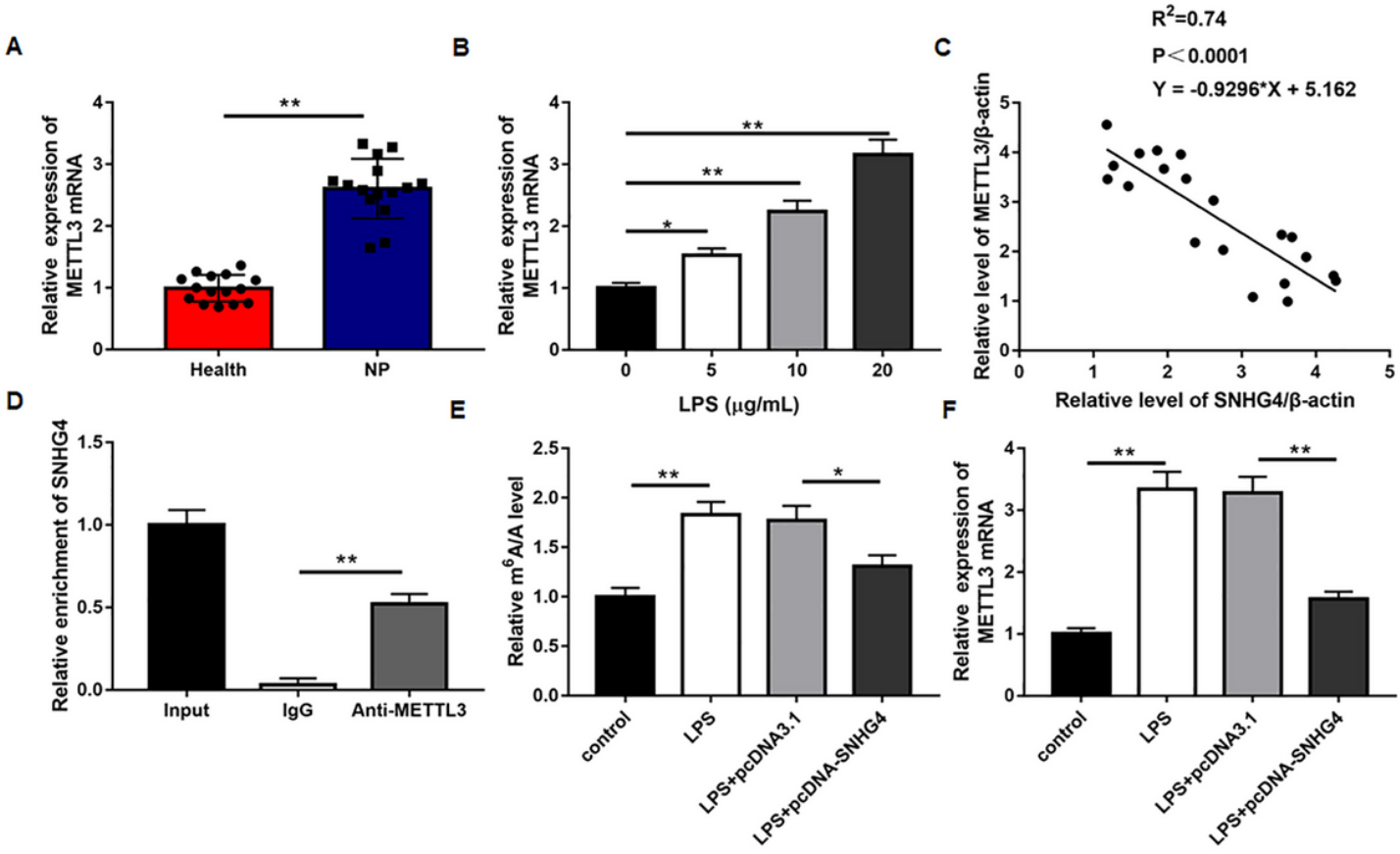

Figure 3

SNHG4 negatively regulated METTL3 expression in human lung fibroblast WI-38 cells. A-B: RT-qPCR was used to detect METTL3 mRNA level in the serum of patients with pneumonia (n = 15) and healthy controls (n = 15), and in WI-38 cells under LPS treatment (0, 5, 10, and 20 μg/mL) for 24 h. C: Pearson correlation test was used to evaluate the relationship between SNHG4 and METTL3. D: The level of SNHG4 in the promoter region of METTL3 was assessed by RIP assay. E: m6A quantitative analysis illustrated the m6A level with or without SNHG4 overexpression. F: RT-qPCR illustrated the METTL3 mRNA expression with LPS administration and pcDNA-SNHG4 transfection. Data were presented as mean ± SEM. N=5, *P < 0.05, **P < 0.01.

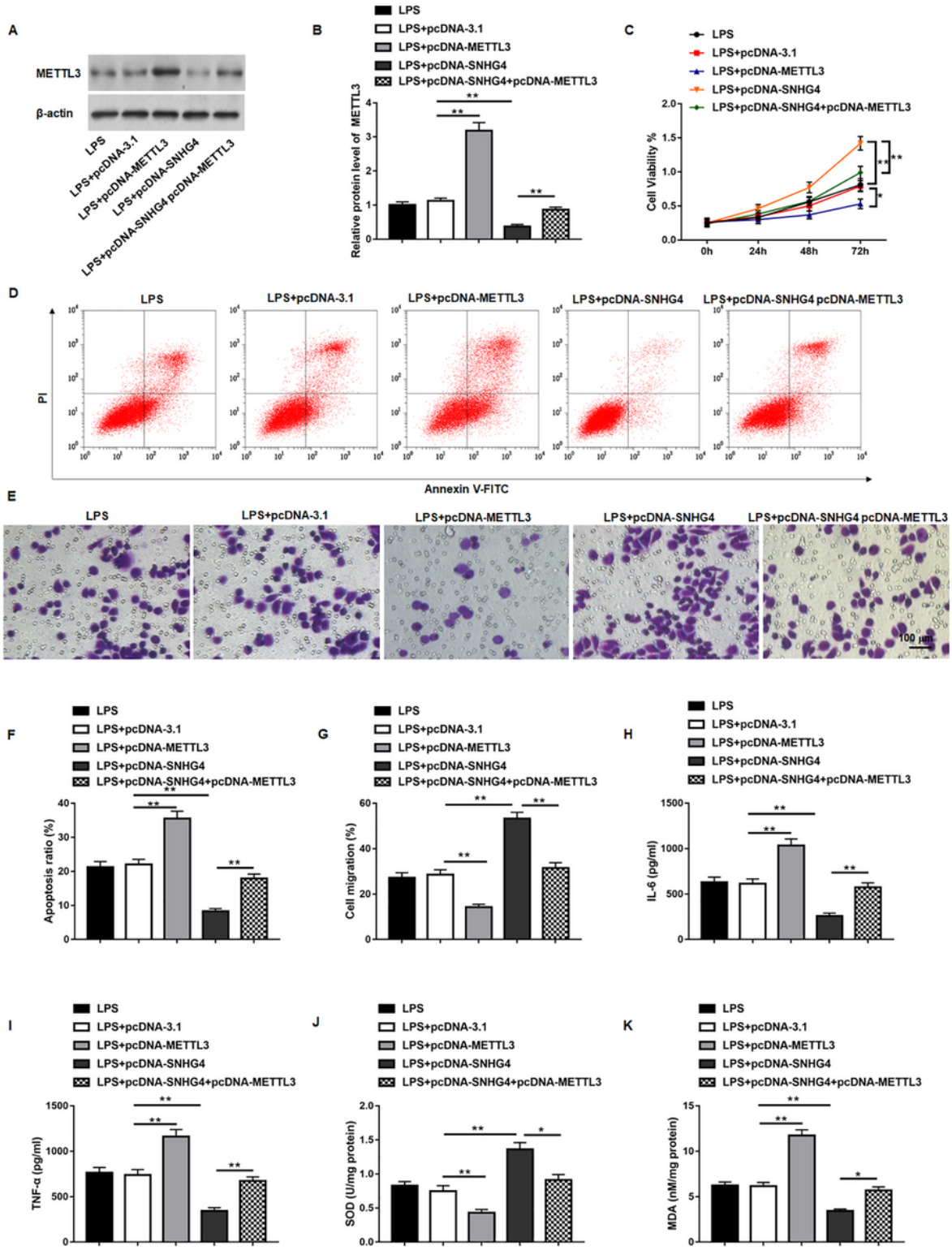

Figure 4

Overexpression of SNHG4 alleviated LPS-induced inflammatory damage by inhibiting METTL3 expression WI-38 cells were transfected alone or together with pcDNA-SNHG4 and pcDNA-METTL3, and then treated with 10 μg/mL of LPS for 24 h. A-B: After LPS stimulation, Western blotting was used to determine the level of METTL3 in WI-38 cells. C: The cell proliferation of WI-38 cells was detected by CCK-8 assay. D and F: The cell apoptosis ratio was determined by flow cytometry. E and G: The cell migration

ability was determined with Transwell assay. H-K: The contents of IL-6, TNF-α, SOD and MDA was detected by ELISA in WI-38 cells. Data were presented as mean ± SEM. N=5, **P < 0.01.

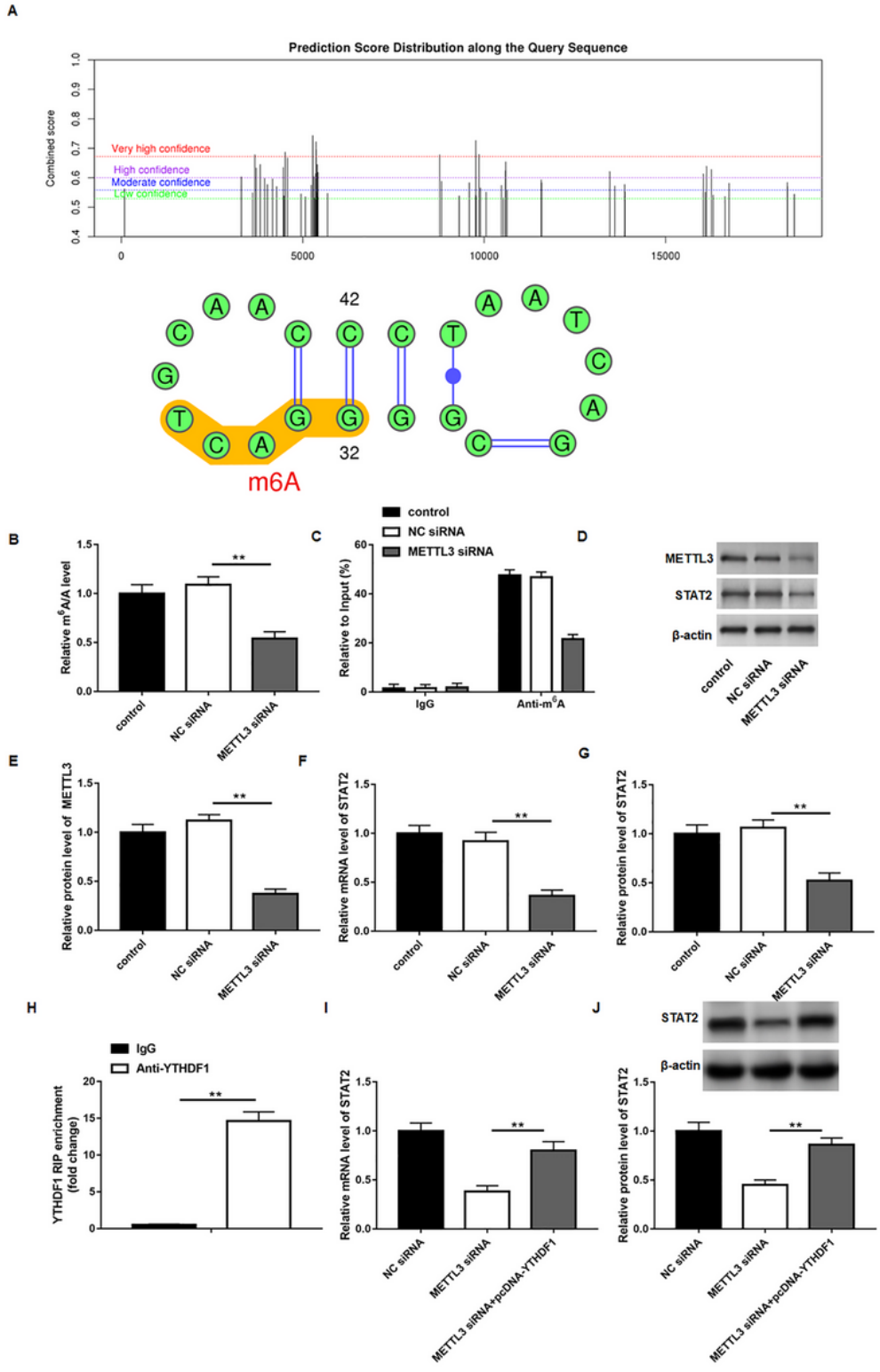

Figure 5

Interference of METTL3 decreases the m6A level of STAT2 mRNA A: Online bioinformatics tools (http://www.cuilab.cn/sramp) revealed the distribution of m6A peak on STAT2 mRNA. B: m6A quantitative analysis illustrated the m6A level with or without METTL3 silencing. C: RIP-qPCR (RNA

immunoprecipitation following qPCR) showed the STAT2 mRNA enrichment precipitated by m6A antibody. D-E and G: Western blotting was used to illustrate the METTL3 and STAT2 protein expression with LPS administration and METTL3 silencing transfection. F: RT-qPCR was used to illustrate the STAT2 mRNA expression with LPS administration and METTL3 silencing transfection. H: RIP analysis of the interaction of STAT2 with YTHDF1 in WI-38 cells transfected with pcDNA-YTHDF1 plasmid. Enrichment of STAT2 with YTHDF1 was measured by qPCR and normalized to input. I: RT-qPCR of STAT2 mRNA in WI-38 cells with or without METTL3 knockdown and transfected with control or pcDNA-YTHDF1 plasmid. J: Western blotting of STAT2 protein in WI-38 cells with or without METTL3 knockdown and transfected with control or pcDNA-YTHDF1 plasmid. Data were presented as mean ± SEM. N=5, **P < 0.01.

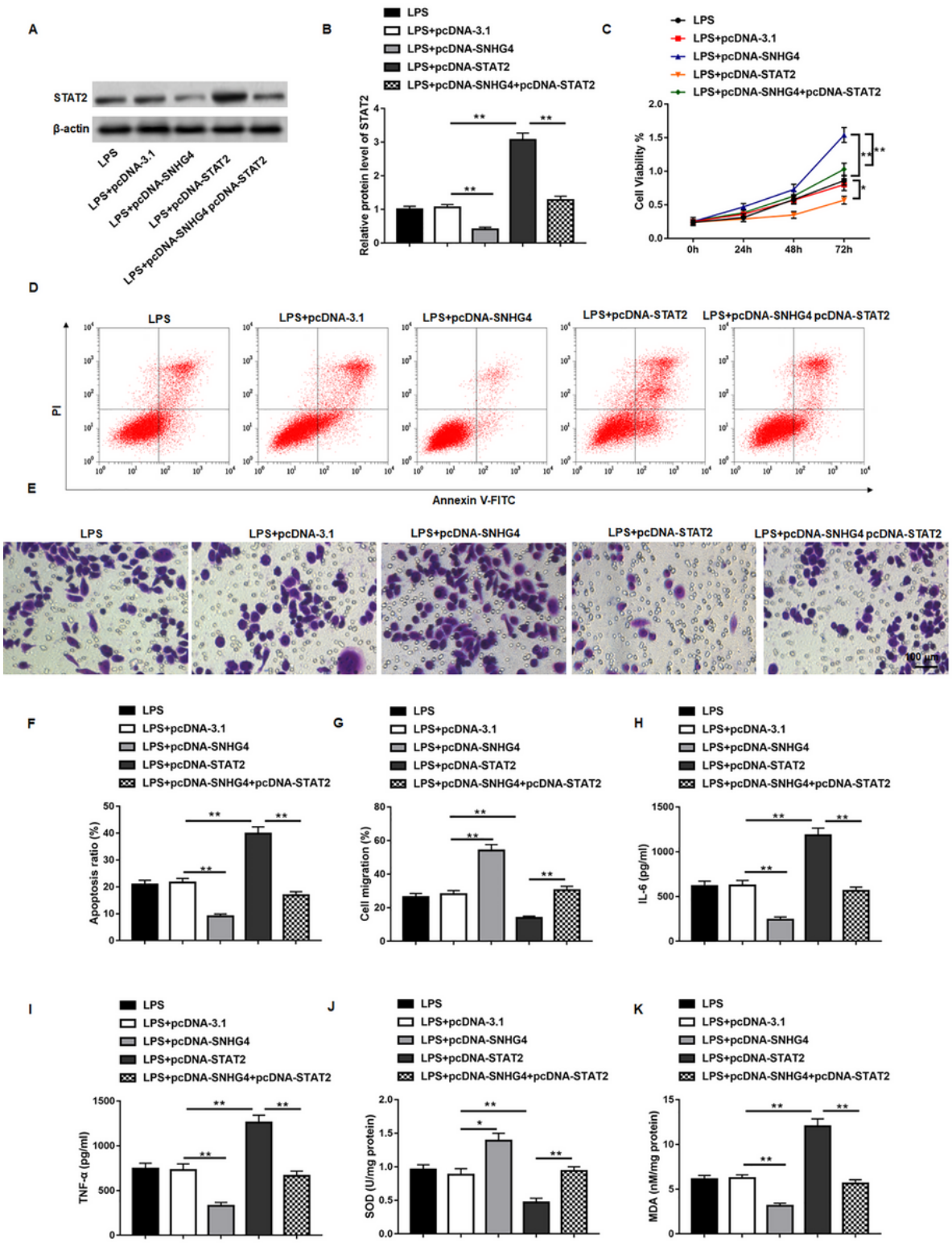

Figure 6

Overexpression of STAT2 reversed the ameliorative effect of SNHG4 upregulated on LPS-induced inflammatory damage WI-38 cells were transfected alone or together with pcDNA-SNHG4 and pcDNA-STAT2, and then treated with 10 μg/mL of LPS for 24 h. A-B: After LPS stimulation, Western blotting was used to determine the level of STAT2 in WI-38 cells. C: The cell proliferation of WI-38 cells was detected by CCK-8 assay. D and F: The cell apoptosis ratio was determined by flow cytometry. E and G: The cell

migration ability was determined with Transwell assay. H-K: The contents of IL-6, TNF-α, SOD and MDA was detected by ELISA in WI-38 cells. Data were presented as mean ± SEM. N=5, *P < 0.05, **P < 0.01.

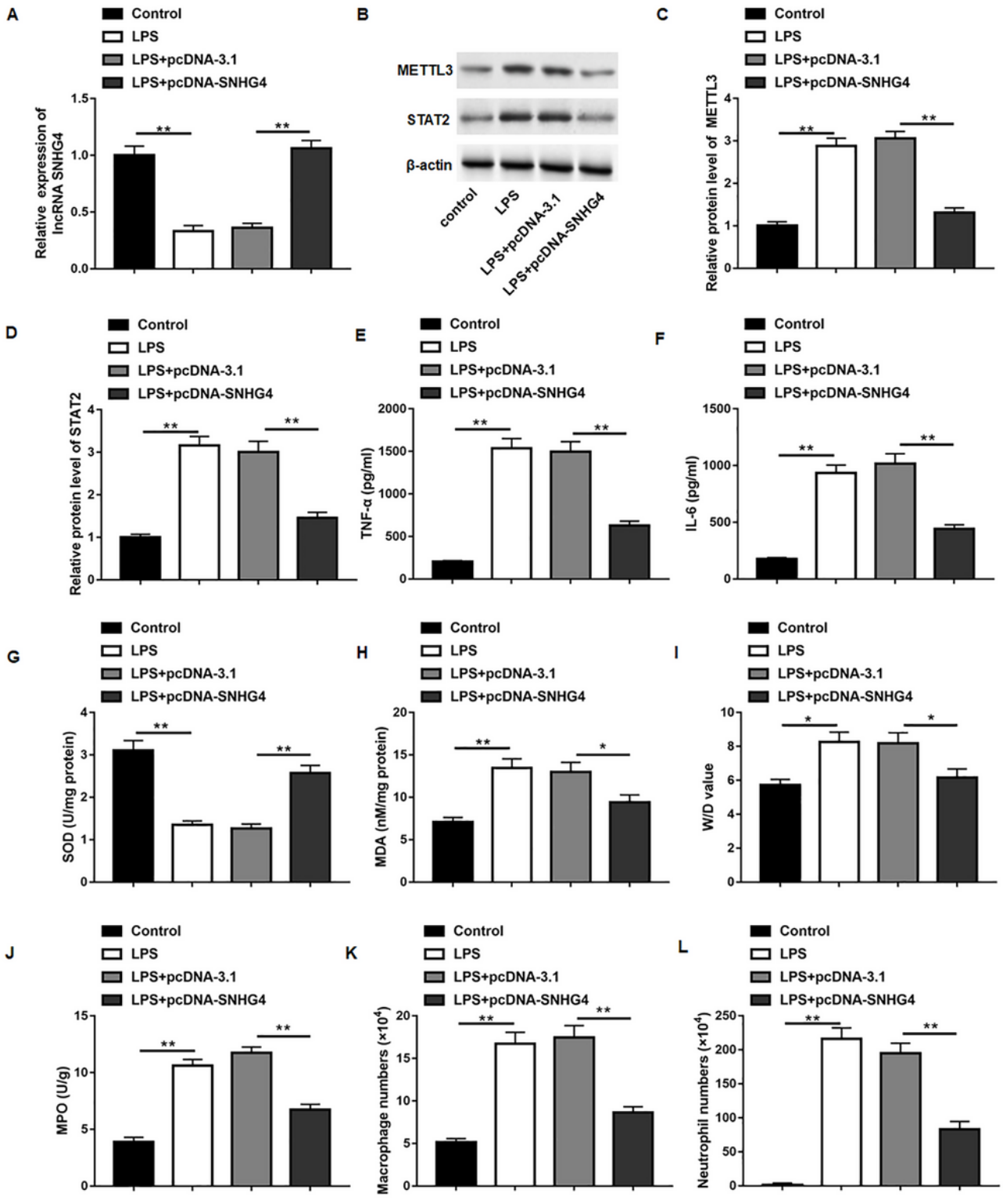

Figure 7

Overexpression of SNHG4 alleviates LPS-induced inflammation and injury in mice pcDNA-3.1 or pcDNA-SNHG4 was intratracheally injected into mice. A: The knockdown efficiency of pcDNA-SNHG4 was determined by RT-qPCR. B-D: Western blotting was used to determine the protein levels of METTL3 and

STAT2 in mouse lung tissues. E-H: The contents of IL-6, TNF-α, SOD and MDA was detected by ELISA in mouse lung tissues. I: Wet dry mass ratio (W/D) of lungs was calculated. J: Myeloperoxidase (MPO) of lungs was examined. K-L: macrophages and neutrophils in alveolar lavage fluid was collected and calculated.